Photochemical & Photobiological Sciences

Accepted Manuscript

This article can be cited before page numbers have been issued, to do this please use: M. E. E. Rodriguez, C. B. Catrinacio, A. Ropolo, V. A. Rivarola and M. I. Vaccaro, *Photochem. Photobiol. Sci.*, 2017, DOI: 10.1039/C7PP00161D.

ROYAL SOCIETY OF CHEMISTRY

rsc.li/pps

Photochemical & Photobiological Sciences

View Article Online
DOI: 10.1039/C7PP00161D

ARTICLE

Received 00th January 20xx,
Accepted 00th January 20xx
DOI: 10.1039/x0xx00000x

www.rsc.org/

A novel HIF-1α/VMP1-Autophagic Pathway Induces Resistance to Photodynamic Therapy in Colon Cancer Cells

M.E. Rodríguez[a,b], C. Catrinacio [b], A. Ropolo [b], V.A. Rivarola [a] and M.I. Vaccaro [b]†.

Colon cancer is the third most frequent cancer and the fourth most common cause of cancer-related mortality worldwide and the standard therapy is surgical resection plus adjuvant chemotherapy. Photodynamic therapy (PDT) has been proposed as adjuvant therapy because it can prevent the tumor recurrence after surgical excision in colon cancer patients. Hypoxia is a common feature in solid tumor and leads to chemo/radio resistance. Recently, it has been shown that in response to hypoxia cell can induce HIF-1α-mediated autophagy to survive in this hostile microenvironment. Moreover, hypoxia and autophagy have been implicated in resistance to antitumor PDT. However, the molecular signals by which HIF-1α induces autophagy in PDT context has not been studied yet. Here we evaluate the interplay between HIF-1α and autophagy as well as the underlying mechanism in the PDT resistance of colon cancer cells. Our study demonstrates that HIF-1α stabilization significantly increases VMP1-related autophagy through binding to hypoxia responsive elements in VMP1 promoter. We show that HIF-1α-induced autophagy increases colon cancer cell survival as well as decreses cell death after PDT. Moreover, here we demonstrate that HIF-1α-induced autophagy is mediated by VMP1 expression, since downregulation of VMP1 by RNA interference strategy reduces HIF-1α-induced autophagy and cell survival after PDT. In conclusion, PDT induces autophagy as a survival mechanism and the induction of the novel HIF-1α/VMP1/autophagic pathway may explain, at least in part, the resistance of colon cancer cells to PDT. The knowledge of the molecular mechanisms involved in PDT resistance may lead to more accurate therapeutic strategies.

[a] Universidad Nacional de Río Cuarto, Departamento de Biología Molecular. Río Cuarto (5800), Córdoba, Argentina.
[b] Universidad de Buenos Aires. CONICET. Facultad de Farmacia y Bioquímica. Instituto de Bioquímica y Medicina Molecular (IBIMOL). Buenos Aires, Argentina.
† Corresponding author. María I. Vaccaro. Email: mvaccaro@ffyb.uba.ar.

Introduction

Colon cancer is the third most frequent cancer and the fourth most common cause of cancer-related mortality worldwide, and the standard curative therapy is surgical resection plus adjuvant chemotherapy[1,2]. Effective treatment modalities are rare in cases of patients with peritoneal carcinomatosis and chemotherapy-resistant tumors[3]. Therefore, novel treatment modalities for such cases are required.

Photodynamic therapy (PDT) is an anti-tumor strategy that is approved for clinical use in a number of countries, for removing early-stage malignancies and palliation of symptoms in patients with late stage tumors[4,5]. PDT involves the use of a light-sensitizing agent, or photosensitizer, followed by illumination of the tumor with visible light; this leads to the production of reactive oxygen species (ROS) that cause direct damage to the tumor as well as the blood vessels supporting the tumor[6]. PDT is a promising anticancer treatment and its major pharmacological effect is to induce cancer cell apoptosis or necrosis through oxidative stress[7].

PDT has been proposed as adjuvant therapy because it can prevent the tumor recurrence after surgical excision in colon cancer patients[8]. In this sense, PDT may be most suitable for the treatment of small tumors or for small areas of persistent tumor[9]. However, the prognosis is poor, particularly for patients with advanced stage tumors, due to the resistance to cell death, in which hypoxic microenvironment potentially plays a critical role[10]. Solid tumors are subjected to hypoxia because they can quickly outgrow the existing vasculature and have decreased access to blood borne nutrients and O_2[11,12]. In this context, the Hypoxia Inducible Factor-1 (HIF-1) is the major regulator of resistance to cell death and proliferation of cancer cells by providing a growth advantage under hypoxic stress[13].

Autophagy is defined as a process of programed cell survival involving the sequestration of cellular components in double membrane structures called autophagosomes, which are degraded after fusion with lysosomes[14]. Autophagy increases cell survival and chemoresistance in different tumor cells[15,16,17]. Recently, it has been shown that in response to hypoxia tumor cells may induce HIF-1-mediated autophagy to survive in that hostile microenvironment[18,19]. Thus, autophagy optimizes nutrient utilization in fast growing cells in response to hypoxia or metabolic stress contributing to cancer cell survival[19]. Hypoxia and autophagy promote resistance to PDT

View Article Online
DOI: 10.1039/C7PP00161D

possibly through apoptosis inhibition in esophageal tumor cells[20,21]. Moreover, inhibition of autophagy induces cell death by potentiating PDT-induced apoptosis in colorectal cancer stem-like cells[22]. However, the interplay between hypoxia and autophagy in PDT context has not been studied yet.

The Vacuole Membrane Protein 1 (VMP1) induces autophagy and plays an essential role in autophagosome formation in mammalian cells[23,24,25,26]. VMP1 also mediates a selective type of autophagy in pancreas with acute pancreatitis, called Zymophagy[27]. Moreover, oncogenic KRAS requires VMP1 expression to induce autophagy[28] and human pancreatic tumor cells activate VMP1-mediated autophagy under chemotherapy agents such as gemcitabine[29].

Here we examine how HIF-1α and autophagy work together to modulate cancer cell response to PDT and the molecular pathways by which HIF-1α induces autophagy to mediate PDT resistance in colon cancer cells. We found that PDT induces autophagy as a survival mechanism in colon cancer cells. We found that HIF-1α stabilization induces a novel HIF-1α/VMP1/autophagy pathway, which in turn, confers resistance to PDT.

Experimental

Cell culture

Human colon cancer CaCo2 cells (ATCC ® HTB-37™) and SW480 (ATCC ® CCL-228™) cells were cultured in Dulbecco's modified Eagle medium (Sigma) supplemented with 10% fetal bovine serum (Internegocios), 100 U ml^{-1} Penicillin, and 100 µg ml^{-1} streptomycin (Sigma) at 37°C in a humidified atmosphere with 5% CO_2. Cells were transfected using FuGENE-6 Transfection Reagent (Promega) as indicated by manufacturer. For $CoCl_2$ treatment, CaCo2 and SW480 cells ($10x10^4$ cell ml^{-1}) were plated in 60-mm dishes. After 24 h the medium was replaced by complete medium with $CoCl_2$ (100, 200 or 400 µM) followed by a 24 h incubation. Cells were treated with 100 nM Rapamacyn, 5 mM 3- methyladenine (3-MA), 100 nM wortmannin (WM) or 10 µM chloroquine (CQ) when indicated. Cell viability was measured by the 3-(4,5-dimethylthiazol-2-yl)-2,5-diphenyltetrazoliumbromide) (MTT) assay.

Chemicals and Photosensitizer

The compound methyl derivative of δ-aminolevulinic acid (Sigma-Aldrich) as a precursor of the photosensitizer protoporphyrin IX (PpIX) was used in this work. A stock solution of 100 mM 5-aminolevulinic acid methyl ester (Me-ALA) was prepared in sterile PBS, from which 1 mM work solution was made employing DMEM culture medium without serum. Cobalt chloride ($CoCl_2$), Rapamycin, 3-MA, WM, CQ, Polyethylenimine (PEI), and Earle's Balanced Salt Solution (EBSS) were purchase from Sigma-Aldrich. Hoechst 33342 (Cell Signaling). All other reagents were of the highest analytical grade available.

Antibodies

The primary antibodies employed were: HIF-1α (R&D), microtubule-associated protein 1A/1B-light chain 3 B (LC3B) (Cell Signaling), p62/SQSTM1 (Cell Signaling), VMP1AtgD (was developed in our laboratory)[23], β-actin (Sigma) and β-tubulin (Sigma). The secondary antibodies used were: horseradish peroxidase (HRP) monoclonal antibody anti-mouse IgG (Cell Signaling), HRP monoclonal antibody anti-rabbit IgG (Cell Signaling), polyclonal goat anti-Rabbit IgG (H+L) Secondary Antibody Alexa Fluor® 594 conjugate (Thermo Scientific™), IRDye® 680LT Goat anti-Rabbit IgG (H + L) (Licor).

Plasmids

5HRE-hCMV-d2EGFP (provided by T. Foster, University of Rochester, Rochester, NY), pRFP-LC3, pLKO.1-shRNAHIF-1α-1 (Provide by Dr. Eric Metzen, University of Duisburg-Essen, Essen, Germany), pCMS3-H1p-EGFP that contains a VMP1 short hairpin RNA construction with the target sequence of VMP1-siRNA developed in our lab[27].

Chromatin Immunoprecipitation (ChIP) Assay

Chromatin immunoprecipitation was conducted following the ChIP kit protocol (Pierce Agarose, Thermo Scientific). Briefly, CaCo2 cells ($3x10^6$) were cross-linked with 1% formaldehyde directly into the media for 10 min at room temperature. The cells were washed and scraped with phosphate-buffered saline and collected by centrifugation at 800g for 5 min at 4 °C, suspended in cell lysis buffer and incubated on ice for 15 min. The pellet was suspended in nuclear lysis buffer and sheared to fragment DNA to 700 bp. Samples were immunoprecipitated using a HIF-1α antibody (R&D), or normal rabbit IgG antibody (Pierce Agarose, Thermo Scientific) overnight at 4 °C on a rotating wheel. Following immunoprecipitation, samples were washed and eluted using the chromatin immunoprecipitation kit in accordance with the manufacturer's instructions. Cross-links were removed at 62 °C for 1.5 h, and immunoprecipitated DNA was purified (Pierce Agarose ChIP Kit, Thermo Scientific) and subsequently amplified by PCR. PCR was performed using three primer sets for the three areas containing potential HIF-1α binding sites in the *VMP1* promoter sequence (Fig. 2D): 1) ACCCAGTGAGACCTCATCTTT (sense) and CACTCCATTGAGATATGGGACA (antisense); 2) GCCCGCACTAAGAGCCTAAC (sense) and CCCCAATTCCCTGAGTTAGTT (antisense); 3) GAGCCCTTGGAGAGGAACTT (sense) and CATGGAGTTGCAGGTAAATAAAAG (antisense). PCR products were visualized by 1.5% agarose gel.
Band images were quantified digitally, using ImageJ software, and data were expressed as relative to Input expression (% of Input).

HRE-EGFP reporter assay

View Article Online
DOI: 10.1039/C7PP00161D

HIF-1 transcriptional activity was assessed using a promoter-reporter plasmid. 5HRE-hCMV-d2EGFP containing five tandem hypoxia response element (HRE) consensus sequences and a human CMV minimal promoter upstream of an enhanced GFP (EGFP) reporter gene that has been previously described by Vordermak and co-workers[30]. CaCo2 cells were transfected employing PEI as transfection reagent. It was mixed 40 µl cold 150 mM ClNa, 1 µg of DNA and finally 1 µl of PEI (1 µg μl^{-1}). This mixture was incubated at 37°C for 15 min and then aggregated to the wells, where cells were growth contained 500 µl of complete medium. After 24 h the transfection medium was replaced by complete medium containing 200 µM $CoCl_2$. The EGFP expression was analyzed 24 h after treatment by confocal fluorescence microscope (FV1000; Olympus).

Immunoblotting

Cells were lysed and proteins were collected with RIPA buffer (150 mM NaCl, 1% Triton X-100, 1% sodium deoxycholate, 0.1% SDS, 10 mM Tris-HCl pH 7.2, 5 mM EDTA, Phosphatase and Protease Inhibitor Cocktail [Sigma-Aldrich]). Protein concentration was determined using the bicinchoninic acid (BCA) protein assay reagent (Pierce). Equal amount of protein was analyzed on SDS-PAGE and transferred to polyvinylidene fluoride membranes (0.22 µm, Millipore). Membranes were then incubated at room temperature for 1 h in blocking buffer (5% low-fat milk powder in Phosphate Buffered Saline (PBS)), and after incubated overnight at 4 °C with primary antibodies. Horseradish peroxidase-conjugated secondary antibody were incubated for 2 h at room temperature. Immunoreactive bands detection was carried out using the enhanced-chemoluminescence (GE Healthcare) according to the manufacturer's instructions. When indicated, IRDye secondary antibodies were used and revealed using Odyssey® SA (Licor). We used ImageJ software to quantify western blot bands. Relative densitometry is expressed as the mean ± SD of 5 different experiments. *t test*: **P < 0.05, **P< 0.01, ***P< 0.001.*

Fluorescence Microscopy

For immunofluorescence, after treatment cells growing on glass slides were fixed with cold methanol and the nonspecific binding was blocked with 3% bovine serum albumin (BSA) in PBS (1% Tween 20). After overnight blocking, the cells were incubated with the primary antibody for 2 h and the signal revealed with Alexa Fluor® 594-conjugated antibody. For nuclear staining, cells were incubated with Hoechst 33342 at room temperature for 10 min. Images were taken by using a confocal microscope (FV1000; Olympus). For quantification of LC3 dots, original images were deconvolved using ImageJ software. Data are expressed as the mean ± SD (dost LC3/cells) of 3 different experiments. *t test*, **P* < 0.05; ***P* < 0.01.

To identify autophagosomes, cells were co-transfected with a red fluorescent protein fused to LC3 (RFP-LC3) and shVMP1-EGFP expression vectors and fixed with 4% p-formaldehyde in PBS for 15 min. We consider an RFP-LC3 cell to have punctate staining when all the red fluorescence is present as punctate and no diffused protein remains. The cells were observed and photographed utilizing a confocal fluorescence microscope (FV1000; Olympus). Percentage of RFP-LC3 Cells with Punctate Staining is the number of cells with punctate staining per 100 fluorescent RFPLC3 transfected cells was determined in three independent experiments. To quantify, the number of fluorescent cells with punctate staining was counted in six random fields representing 100 fluorescent cells and expressed as the mean S.D. of combined results. We consider an RFP-LC3 cell to have punctate staining when all the red fluorescence is present as punctate and no diffused protein remains. Experimental groups were compared using *t test* for pairwise comparison (n=3, ****p* < 0.001).

Photodynamic therapy

CaCo2 and SW480 cells (12 x 10^4 cells ml^{-1}) were seeded in 96-wells plates and kept in the incubator at 37 °C overnight. Cells were incubated with Me-ALA 1mM for 4 h and then irradiated at 1, 2, 3, 4 and 5 J cm^{-2} (n=8). Cells were irradiated employing a monochromatic light source (635 ± 17 nm) with a multi-LED system (coherent light) at irradiation intensity of 1.65 mW cm^{-2} (as measured by Coherent Lasermate power meter). The culture medium was changed by complete medium. After 24 h of treatment, 10 µl of MTT stock solution were added to each well containing 100 µl of complete medium. Cells were incubated with MTT for 4 h and formazan crystals were suspended in DMSO. Absorbance of the samples was read with a Multiskan FC photometer (Thermo Scientific) at 540 nm. The absorbance of control cells was considered as 100% of viability. When indicated, cells were subjected to PDT and treated with 100 nM WM, 5mM 3-MA, 10 µM CQ, 100 nM Rapamycin, 200 µM $CoCl_2$, or transfected with shHIF-α or shVMP1 expression vectors. After 24 h, cell viability was measured by MTT assay. Cytotoxicity was expressed as viability percentage of the control. When autophagic activator/inhibitors were employed in combination with PDT, optical density values from activator/inhibitor-treated cells without PDT were defined as 100 % of viability. Analysis was carried out on normalized data by one-way ANOVA followed by Bonferroni's multiple comparisons test. Data are expressed as the mean ± SD of 5 different experiments. **P* < 0.05. When indicated, cell death was quantified with Trypan Blue Exclusion Assay. Briefly, after 24 h of Me-ALA PDT, cells were trypsinized and incubated with 0.4% (w/v) Trypan Blue at room temperature for 10 min. Cells with Trypan blue uptake were counted as dead cells on a haemocytometer. Each individual experiment was repeated for three times.

Statistical analysis

View Article Online
DOI: 10.1039/C7PP00161D

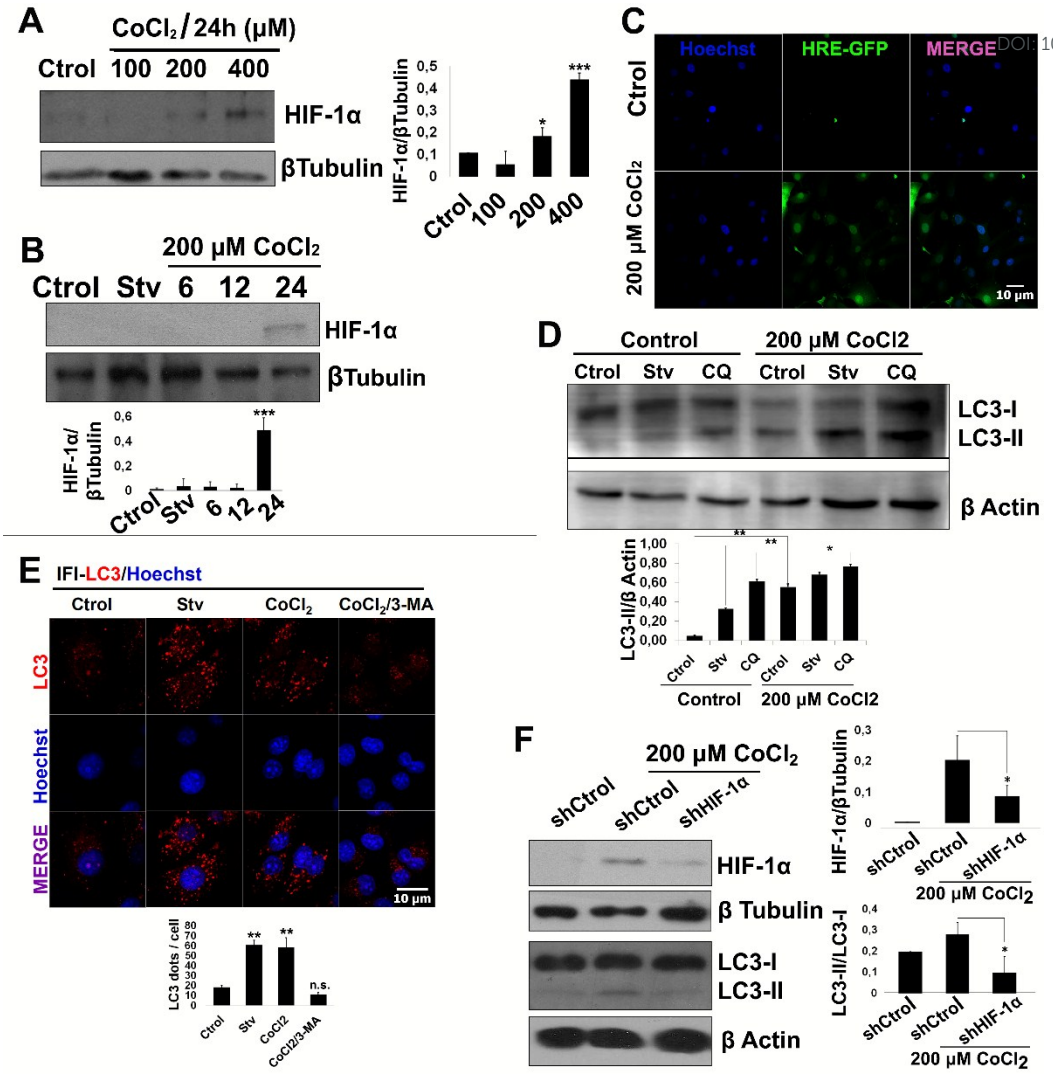

Figure 1. HIF-1α induces autophagy in colon cancer cells. **A)** CaCo2 cells were treated with different doses of $CoCl_2$ (100, 200 or 400 μM) for 24 h and the expression of HIF-1α was detected by western blot. Relative densitometry (HIF-1α/βTubulin) is shown in right panel (n=5, *P<0,05 vs Control, ***p<0,001 vs. Control). **B)** Cells were treated with 200 μM $CoCl_2$ for 6, 12 or 24 h and the expression of HIF-1α was detected by western blot. Lower panel shows relative densitometry (HIF-1α/βTubulin) (n=**5**, ***p<0,001 vs Control). **C)** CaCo2 cells were transiently transfected with p5HRE-EGFP plasmid and treated with 20**0** μM $CoCl_2$ for 24 h. The transcriptional activity of HIF-1α was determined analyzing EGFP expression using confocal microscope. Bar scale = 10 μm **D)** CaCo2 cells were incubated in control medium (Ctrol); starving medium (Stv) or chloroquine (CQ) with or without 200 μM $CoCl_2$ and LC3 expression was detected by western blot. Starvation was used as a positive control of autophagy and CQ was used to inhibit autophagic flux. Lower panel shows relative densitometry (LC3-II/βActin) (n=5, p<0,05 **p<0,01). **E)** CaCo2 cells were starved (Stv) as autophagy positive control, treated with 200 μM $CoCl_2$ or 200 μM $CoCl_2$ plus the autophagy inhibitor 3-methyladenine (3-MA). Autophagic vesicles were detected by indirect immunofluorescence (IFI) of LC3. Images were obtained using confocal microscopy. Representative images show the punctate LC3 in the cytoplasm indicating autophagy. Bar scale = 10 μm. Quantification of number of LC3 dots per cells is shown in lower panel (n=5, n.s.=non-significant, **p<0,01 vs Control). **F)** Cells were transiently transfected with control vector (shCtrol) or shRNAHIF-1α vector (shHIF-1α), and treated with 200 μM $CoCl_2$ during 24 h. The expression of HIF-1α and LC3 were analyzed by western blot. Relative densitometries are shown on the right panel (HIF-1α/βTubulin; LC3-II/LC3-I) (n=**5;** *p<0,05).

The results are expressed as mean ± SD. The present studies comply with the recommendations on experimental design and analysis in pharmacology[31]. We performed a minimum of five independent experiments, where individual data points were based on at least technical duplicates each. Different kinds of ANOVA models were applied to explore differences between groups of quantitative data. Repeated measures ANOVA were used to test for related, not independent groups of quantitative data. Two-way ANOVA was employed to compare the mean differences between groups that have been split on two independent variables. Two-way ANOVA with repeated measures on one of the factors was applied to test differences in experiments where the quantitative dependent variable was measured over two or more-time points. Bonferroni was used as post hoc test. P values less than 0.05 were considered statistically significant. Statistical analysis of data was performed using GraphPad Prism 6.

Results

HIF-1α induces autophagy in colon cancer cells

To explore whether HIF-1α is involved in autophagy induction in colon cancer cells we used the HIF-1α stabilizing agent cobalt chloride ($CoCl_2$). $CoCl_2$ promotes the stabilization of HIF-1α, which is normally hydroxylated and degraded by

View Article Online
DOI: 10.1039/C7PP00161D

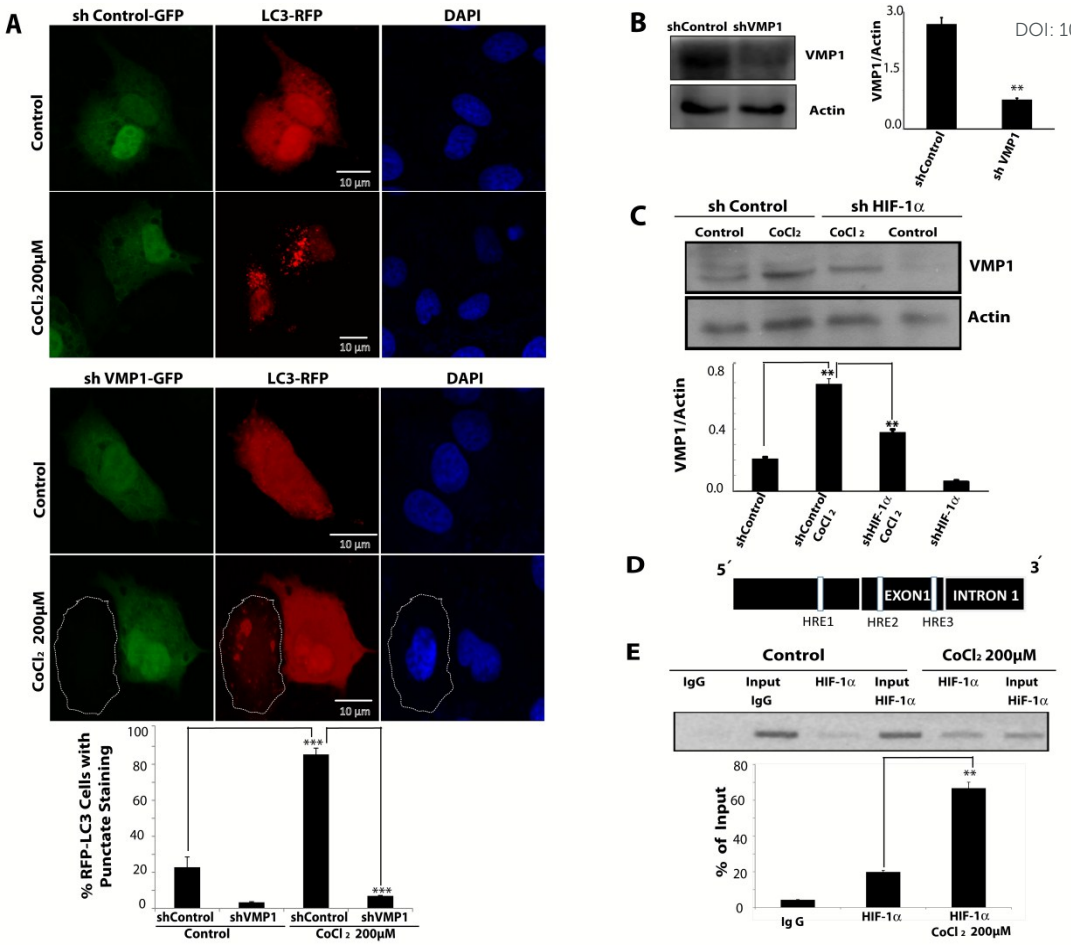

Figure 2. Autophagy induced by HIF-1α is mediated by the expression of autophagy related-protein VMP1. **A)** CaCo2 cells were transiently co-transfected with RFP-LC3 and shVMP1-EGFP expression vectors, and they were treated with 200 µM $CoCl_2$ for 24 h. RFP-LC3 distribution was detected using confocal microscopy. Representative images show the punctate RFP-LC3 in cells EGFP- vs. EGFP+. White circle shows shVMP1-EGFP non-transfected cell. Bar scale = 10 µm. Quantitation represents percentage of RFP-LC3 cells with punctate staining (n=5, ***P<0,001). **B)** CaCo2 cells were transfected with shControl or shVMP1 expression vector. VMP1 expression was detected by western blot Relative densitometry (VMP1/Actin) is shown in right panel (n=5, **P<0.01). **C)** CaCo2 cells were transfected with shHIF-1α or shControl, and treated with 200 µM $CoCl_2$ during 24 h. Control cells were incubated in normal medium. VMP1 expression was detected by western blot. Relative densitometry (VMP1/Actin) is shown in lower panel (n=5, **P<0.01).**D)** Scheme showing 3 HRE consensus elements found in position 59704668-59708628 on chromosome 17 of the human genome, which includes exon 1, intron 1 and 2800 bp 5´upstream sequence of exon 1 from vmp1 gene. **E)** Control CaCo2 cells and treated with 200 µM $CoCl_2$ for 24 h were lysed, and ChIP assay was performed using a HIF-1α antibody. IgG is a negative control. PCR was performed using specific set of primers as described under "Methods". The positive amplicon for the ChIP assay was located 579 bp to 765 bp downstream of the beginning of the first intron (HRE3). Input is total DNA of VMP1-promoter loading for each condition. Quantitation represents percentage of HIF-1α antibody bound to the VMP1-promoter relative to input (% of Input) (n=5, **P<0,01).

proteasome system in presence of molecular oxygen[32]. To standardize experimental conditions and ensure HIF-1α expression in our cell model, CaCo2 cells were treated with 100, 200 and 400 µM $CoCl_2$ for 24 h and HIF-1α levels were evaluated by western blot. As shown in Figure 1A, HIF-1α expression increases under 200 µM $CoCl_2$ treatment. We then evaluated the time required for stabilization of HIF-1α. CaCo2 cells were treated with 200 µM $CoCl_2$ and HIF-1α levels were evaluated by immunoblot after 6, 12 and 24 h post treatment. As shown in Figure 1B, HIF-1α expression increases after 24 h of $CoCl_2$ treatment. Next, the transcriptional activity of HIF-1 following $CoCl_2$ treatment was studied. After dimerization of subunits α and β, HIF-1 recognizes HRE sequences, binds to promoter DNA and modulates transcription of its target genes[33]. For this reason, we used the p5HRE-EGFP plasmid, which is a reporter vector of HIF-1 activity, that produces EGFP expression when HIF-1 is active[34]. CaCo2 cells were transiently transfected with p5HRE-EGFP, treated with 200 µM $CoCl_2$, and EGFP fluorescence was determined by confocal microscopy after 24 h. Figure 1C shows that CaCo2 cells induce EGFP expression after $CoCl_2$ treatment. These results demonstrate that HIF-1 is stabilized and activated after 24 h $CoCl_2$ treatment in colon cancer cells.

To evaluate if HIF-1α promotes autophagy, we analyzed LC3 processing by immunoblot following $CoCl_2$ treatment. During autophagy, the LC3 protein is processed from 18 kDa to 16 kDa form, which is recruited to autophagosomal membrane.

View Article Online
DOI: 10.1039/C7PP00161D

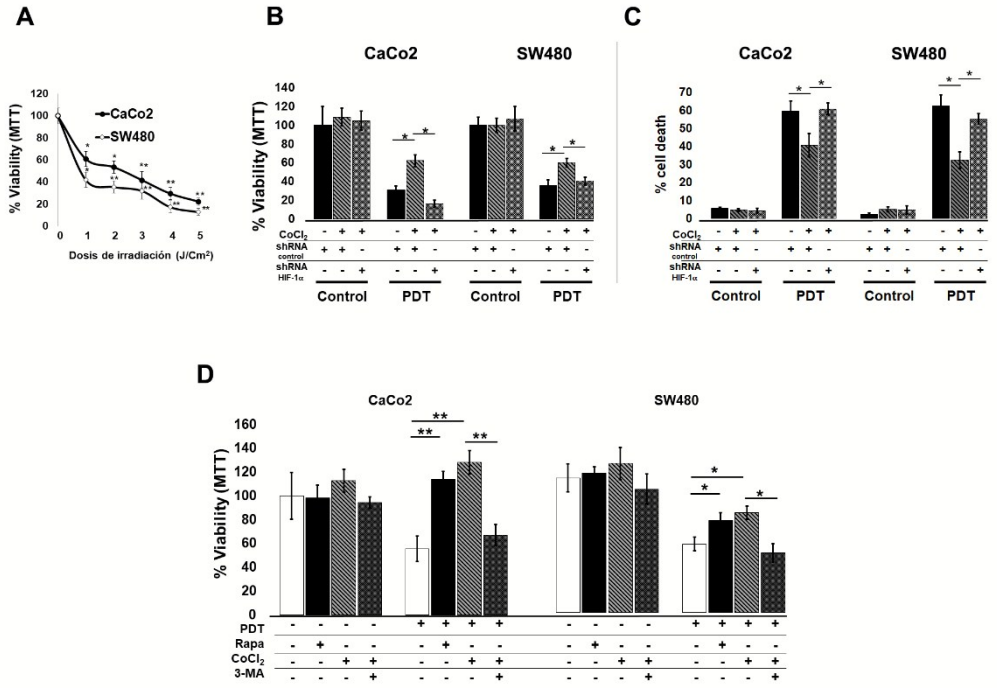

Figure 3. HIF-1-induced autophagy confers resistance to PDT. A) CaCo2 and SW480 cells were incubated with 1 mM Me-ALA for 4 h followed by irradiation with different light doses (1, 2, 3, 4 or 5 J cm-2). Cell viability was evaluated by MTT assay 24 h after irradiation. The control group (0J cm-2) was considered 100% of viability for each cell line. Data were obtained from five independent experiments and are shown as mean ± SD. (*p<0.05, **p<0.01). **B)** Cell survival rate of CaCo2 and SW480 cells transiently transfected with control vector (shCtrol) or shRNAHIF-1α vector (shHIF-1α) and pre-treated with 200μM $CoCl_2$. All groups were treated or not with Me-ALA/PDT (Irradiation doses: CaCo2: 3J cm-2; SW480: 2J cm-2). Cell viability was assessed by MTT 24 h after irradiation. The percentage of viability was calculated for each group treated with PDT, relative to their control (non-treated with PDT). Data were obtained from five independent experiments and are shown as mean ± SD (*p< 0.05). **C)-**CaCo2 and SW480 cells were transiently transfected with control vector (shCtrol) or shRNAHIF-1α vector (shHIF-1α) and pre-treated with 200μM $CoCl_2$. The groups were treated or not with Me-ALA/PDT (Irradiation doses: CaCo2: 3J cm-2; SW480: 2J cm-2). Cell death was determined using trypan blue exclusion assay 24 h after irradiation. Quantitation represents percentage of trypan blue positive cells (dead cells). Data are shown as mean ± SD of five independent experiments. (*p<0.05, **p<0.01). **D)** Cell survival rate of CaCo2 and SW480 cells pre-treated with 100 nM Rapamycin (Rapa), 200 μM CoCl2 or 200 μM CoCl2 plus10 mM 3-methyladenine (3-MA) and treated or not with Me-ALA/PDT. The percentage of viability was calculated for each group treated with PDT, relative to their control (non-treated with PDT). Data were obtained from five independent experiments and are shown as mean ± SD (*p< 0.05; **p<0,01).

Therefore, increased LC3-II levels correlates with autophagy activation[35]. CaCo2 cells were incubated in control conditions and treated with 200 μM $CoCl_2$. Starving medium was used to induce autophagy and CQ treatment to inhibit autophagy flux. Protein extracts were evaluated by immunoblot after 24 h of incubation. Figure 1D shows that after HIF-1α stabilization, autophagy was induced as is demonstrated by increased LC3-II levels. Moreover, the use of CQ in combination with $CoCl_2$ treatment induces LC3-II accumulation compared to $CoCl_2$ or CQ alone treatment, supporting that autophagy flux is actually induced by chemically HIF-1 activation. Next, we performed immunofluorescence of LC3 in cells incubated with $CoCl_2$. Starvation was used as positive control of autophagy induction. Also, we used 3-MA, an inhibitor of PI3K Class III in the initial steps of autophagy as a negative control. Figure 1E shows the recruitment of LC3 in colon cancer cells under $CoCl_2$ treatment, which is abolished by 3-MA. To further confirm the role of HIF-1α in $CoCl_2$-induced autophagy, cells were transfected with shRNAHIF-1α or shRNA-control vector before $CoCl_2$ treatment and LC3 expression was analyzed by western blot. As shown in Figure 1F, LC3-II levels are reduced when HIF-1α is downregulated. Together, these data suggest a key role of HIF-1 in autophagy regulation in colon cancer cells.

Autophagy induced by HIF-1α is mediated by the expression of autophagy related-protein VMP1

HIF-1α-induced autophagy has been reported in a wide variety of cancer cell lines[36,37], including colon cancer cells[38]. However, the molecular mechanisms involved in HIF-1α-induced autophagy remains to be clarified.

VMP1 is an autophagosomal transmembrane protein that triggers autophagy even under nutrient-rich conditions[23]. To determine whether $CoCl_2$ treatment induces VMP1-mediated autophagy, we evaluate LC3 recruitment in CaCo2 cells transiently co-transfected with RFP-LC3 and shVMP1-EGFP and treated with $CoCl_2$. Figure 2A shows RFP-LC3 recruitment is not observed when VMP1 is downregulated in cells co-expressing shVMP1-EGFP and RFP-LC3, indicating that VMP1 is required

View Article Online
DOI: 10.1039/C7PP00161D

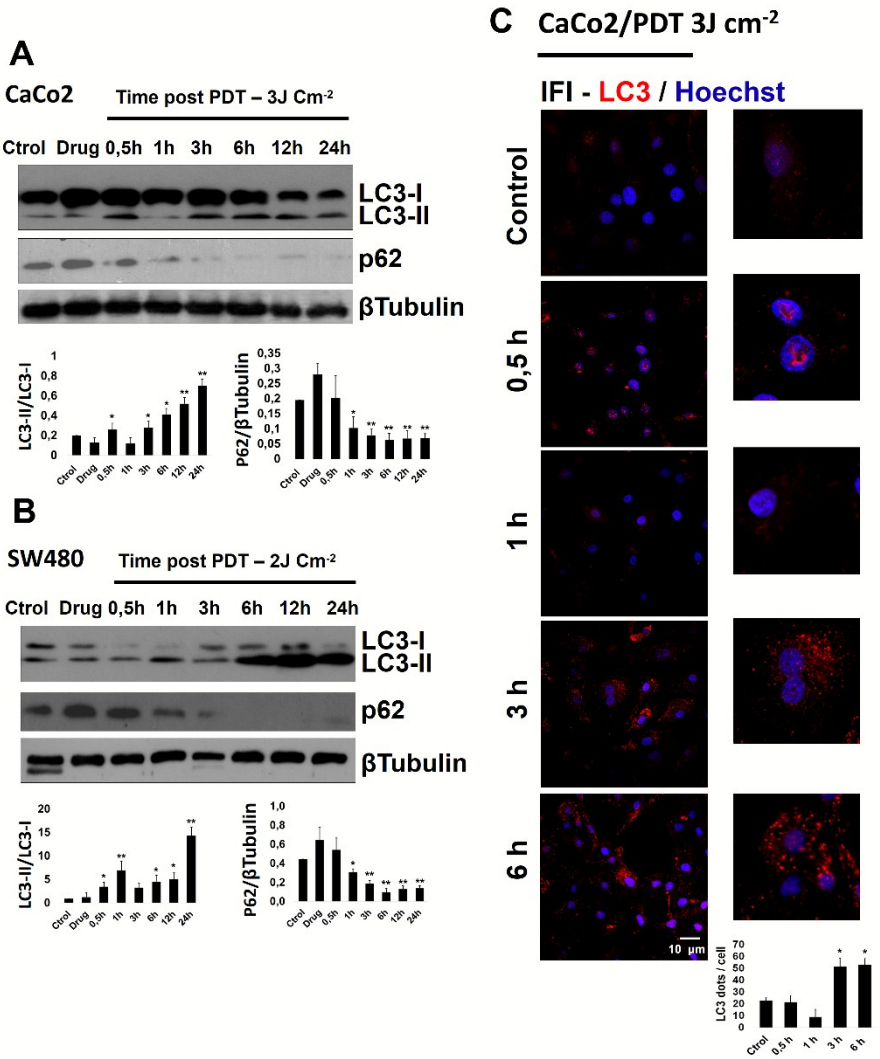

Figure 4. Photodynamic therapy induces autophagy in colon cancer cells. A, B) CaCo2 and SW480 cells were treated with 1 mM Me-ALA/PDT and protein extraction was realized at different time point after therapy. LC3 and p62/SQSTM1 expression were analyzed by western blot (Ctrol: untreated cells; Drug: Me-ALA without irradiation). Lower panel shows relative densitometry (LC3-II/LC3I and P62/βTubulin). (n=5, *p< 0.05 vs Control; **p<0,01 vs Control). **C)** CaCo2 cells were incubated with 1 mM Me-ALA for 4 h and then irradiated with 3 J cm-2. Autophagic vesicles (AV) were detected by Indirect Immunofluorescence (IFI) of LC3. Images were obtained by confocal microscope. Representative images showed the punctate LC3 at different time points after treatment. Lower panel shows the quantification of number of LC3 dots/cells (n=5, *p< 0.05 vs Control ; **p<0,01 vs Control)

for autophagy induction in response to HIF-1α stabilization. Figure 2B shows downregulation of VMP1 by shVMP1-EGFP.

We then explore whether HIF-1α is able to regulate the expression of VMP1. CaCo2 cells treated with 200 µM $CoCl_2$ during 24 h show increased VMP1 expression compared to untreated control cells. Moreover, cells treated with $CoCl_2$ after silencing of HIF-1α with a specific shHIF-1α show significant reduction in VMP1 expression (Fig. 2C). The presence of three putative HIF-1α consensus-binding sites on human VMP1 promoter sequence given by in silico analysis, suggests that HIF-1α is a potential transcription factor regulating VMP1 gene expression (Fig. 2D). Given that the activity of HIF-1α is necessary to induce VMP1 expression in $CoCl_2$ treated cells, we evaluated whether this effect is due to a direct binding of HIF-1α to VMP1 promoter. We performed a ChIP assay using chromatin immunoprecipitation from CaCo2 cells with a specific HIF-1α antibody and specific primers for putative binding sites of this factor in the VMP1 promoter sequence. Figure 2E shows positive amplification signal of HIF-1α to putative binding sites in VMP1 promoter in anti-HIF-1α precipitates from CaCo2 cells submitted to 200 µM $CoCl_2$ treatment. These results demonstrate that HIF-1α binds directly to a region located 579 bp to 765 bp downstream of the beginning of the first intron of VMP1 gene and confirm that HIF-1α is able to regulate VMP1 gene expression. Under $CoCl_2$ treatment, the percentage of input increases 3.4-fold compared to untreated cells. Together, these results demonstrate a new mechanism of autophagy induction in human tumor cells, in which VMP1 is a novel direct target of HIF-1α.

View Article Online
DOI: 10.1039/C7PP00161D

transfected with shRNA HIF-1α to induced HIF-1α

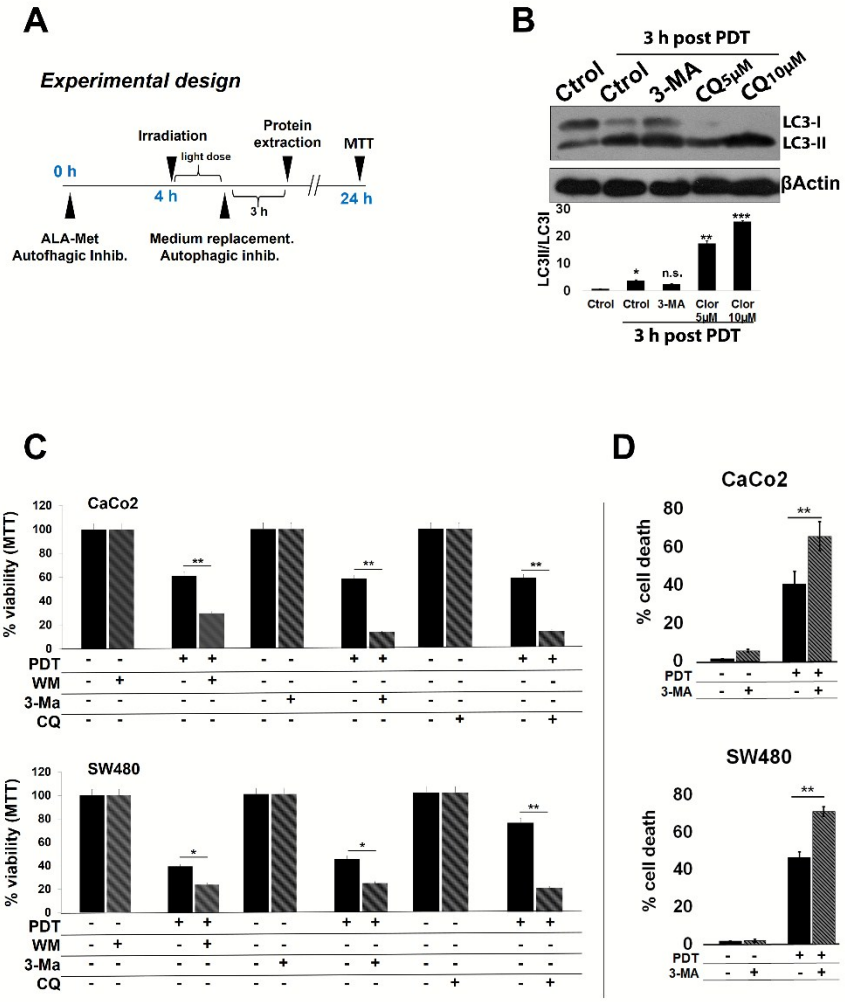

Figure 5. Autophagy induced by PDT promotes resistance in colon cancer cells. A) Schema of experimental design. **B)** CaCo2 cells were pre-treated with 5 mM 3-methyladenine (3-MA) or chloroquine (CQ) (5 µM or 10 µM) before Me-ALA/PDT treatment. Protein extraction was realized at 3 h after PDT and LC3 level was evaluated by western blot. Lower panel shows relative densitometry (LC3-II/LC3I) (n=5, n.s.= non-significant, *p< 0.05 vs Control; **p<0,01 vs Control, ***p<0,001 vs Control). **C)** CaCo2 and SW480 cells incubated with 10 µM wortmannin (WM), 5 mM 3-MA or 10 µM CQ were treated with PDT. After irradiation, the medium was replaced by medium with autophagic inhibitors for 4 h. Cell viability was evaluated by MTT assay 24 h after irradiation. Values are expressed as percentage of viability relative to control group without PDT. Data were obtained from five independent experiments and are shown as mean ± SD. (*p< 0.05; **p<0, 01). **D)** CaCo2 and SW480 cells were incubated with 5 mM 3-MA and treated with PDT (Irradiation doses: CaCo2: 3J cm-2; SW480: 2J cm-2). After irradiation, the medium was replaced by medium with autophagic inhibitor for 4 h. Cell death was assessed by trypan blue exclusion assay 24 h after irradiation. Quantitation represents percentage of trypan blue positive cells (dead cells). Data are expressed as mean ± SD of five independent experiments. (*p<0.05, **p<0.01).

The HIF-1-induced autophagy confers resistance to PDT

Colon tumor cells are normally under hypoxic conditions and activate HIF-1α to survive in this hostile microenvironment. To investigate the effect of HIF-1α activation in PDT context, we first performed a dose-response curve of Me-ALA/PDT in CaCo2 and SW480 cells. Me-ALA/PDT induces significant cytotoxicity in light-dose dependent manner as indicate the MTT assay (Fig. 3A). Sub-lethal dose (3 J cm-2 in CaCo2 cells and 2 J cm-2 in SW480 cells) was used for all the following experiments.

We then evaluated the role of HIF-1α in cell survival after PDT. Cells were incubated with 200 µM $CoCl_2$ and transiently downregulation or shRNA Control. As shown in the Figure 3B, HIF-1α stabilization significantly increases cell survival rate in both cell lines after PDT. Interestingly, HIF-1α downregulation sensitizes CaCo2 and SW480 cells to PDT effect. Moreover, we evaluated cell death by trypan blue exclusion assay 24 h after irradiation. As shown in Figure 3C, the percentage of cell death is reduced in cells treated with $CoCl_2$, and HIF-1α downregulation significantly increases cell dead in both cell lines. These results suggest that HIF-1α mediates resistance to PDT in these cells.

View Article Online
DOI: 10.1039/C7PP00161D

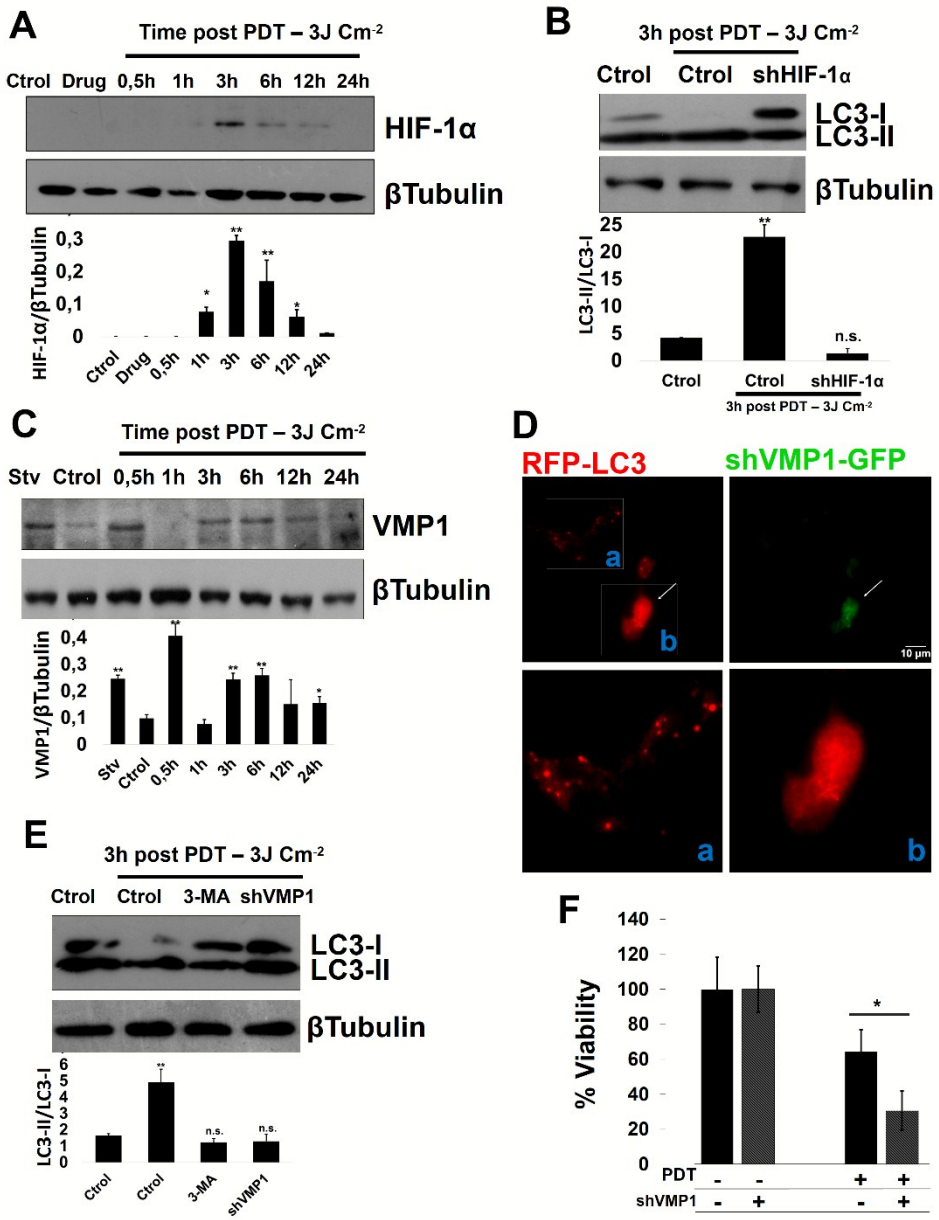

Figure 6. HIF-1α /VMP1/autophagy pathway mediates PDT resistance in colon cancer cells. **A)** CaCo2 cells were treated with Me-ALA/PDT and protein extraction was realized at different time point after therapy. HIF-1α expression was analyzed by western blot (Ctrol: untreated cells; Drug: Me-ALA without irradiation). Lower panel shows relative densitometry (HIF-1α/βTubulin). (n=5, *p<0.05 vs Control; **p<0,01 vs Control). **B)** CaCo2 cells were transiently transfected with control vector (Ctrol) or shRNAHIF-1α vector (shHIF-1α) and treated with Me-ALA/PDT. 3h post therapy, LC3 expression was detected by western blot. Lower panel shows relative densitometry (LC3-II/LC3I). (n=5, n.s. = non-significant, **p<0,01 vs Control). **C)** CaCo2 cells were treated with Me-ALA/PDT and protein extraction was realized at different time point after therapy. VMP1 protein expression was evaluated by western blot (Ctrol: untreated cells; Stv: Starved cells). Lower panel shows relative densitometry (VMP1/βTubulin) (n=5, *p<0.05 vs Control, **p<0,01 vs Control). **D)** CaCo2 cells co-transfected with shVMP1-EGFP and RFP-LC3 expression vectors were treated with Me-ALA/PDT. RFP-LC3 distribution was evaluated and photographed by fluorescence microscope 3h post therapy. Representative images show the punctate RFP-LC3 in cells EGFP- (*inset a*) vs EGFP+ (*inset b*). White arrow shows shVMP1-GFP-expresing cells. Bar scale = 10 µm. **E)** Cells were transiently transfected with control vector (Ctrol) or shVMP1-EGFP vector (shVMP1) and treated with Me-ALA/PDT. LC3 expression was detected 3 h post therapy by western blot. Lower panel shows relative densitometry (LC3-II/LC3I). (n=5, p**p<0,01 vs Control). **F)** Cell survival rate of CaCo2 cells transiently transfected with control or shVMP1-EGFP vector before Me-ALA/PDT. Cell viability was assessed by MTT 24 h after irradiation. The percentage of viability was calculated for each group treated with PDT, relative to their control (non-treated with PDT).Data were obtained from five independent experiments and are shown as mean ± SD. (*p< 0.05).

Then, we explored the role of HIF-1α-mediated autophagy induced by $CoCl_2$ treatment in colon cancer cells after PDT. We treated CaCo2 and SW480 cells with rapamycin to induce autophagy; with $CoCl_2$, and with $CoCl_2$ plus 3-MA to inhibit autophagy. After 24 h of incubation, we evaluated cell viability and found that autophagy, either induced by rapamycin or $CoCl_2$ treatment, promotes resistance to cell death under PDT (Fig. 3D). Remarkably, the inhibition of autophagy in cells treated with $CoCl_2$ sensitizes both cell lines to photodynamic effect. Together, our findings suggest that HIF-1α-induced autophagy is able to promote cancer cell resistance to PDT.

View Article Online
DOI: 10.1039/C7PP00161D

Autophagy induced by PDT promotes resistance in colon cancer cells

Above we demonstrated that autophagy induced by HIF-1α confers resistance to PDT. Next, we evaluated the effect of PDT on autophagy. CaCo2 and SW480 cells were treated with Me-ALA/PDT and autophagic flux was evaluated by immunoblot and fluorescence microscopy analysis in a time course after treatment. As shown in Figure 4A and 4B, LC3-II levels increase after 3 h and 30 min PDT in CaCo2 and SW480 cells, respectively. In order to evaluate autophagic flux, we determined the integrity of p62/SQSTM1, which is selectively degraded by autophagy[39]. Accordingly, decreased levels of p62/SQSTM1 expression are observed in both cell lines in a time dependent manner, indicating increased autophagic flux after treatment. Moreover, LC3 aggregates in puncta since 30 min after PDT compared to control cells without treatment (Fig. 4C). Therefore, PDT induces autophagy in colon cancer cells.

We then studied the role of autophagy in PDT context. CaCo2 and SW480 were incubated with Me-ALA and several inhibitors of autophagy for 4 h and LD50 irradiation dose was applied. Figure 5A shows the experimental design. As shown in figure 5B, 3-MA blocks the LC3-II conversion and CQ pre-treatment induces an exacerbated accumulation of LC3-II form confirming that autophagic flux is induced under PDT in colon cancer cells. Next, we evaluated cell viability by MTT and trypan blue exclusion assay. Figure 5C shows that autophagy inhibition with 3-MA, wortmanin (WM) or CQ photosensitizes both cell lines to photo-damage effects. Furthermore, as shown in Figure 5D, the percentage of cell death was higher when autophagy was inhibited in both cell lines. Altogether, our results indicate that PDT-induced autophagy mediates resistance to PDT in colon cancer cells.

HIF-1α /VMP1/autophagy pathway mediates PDT resistance in colon cancer cells

So far, we demonstrated that HIF-1α/VMP1/autophagy pathway is induced by $CoCl_2$ in colon cancer cells and confers resistance to PDT. Next, we evaluated the effect of PDT on this new pathway. HIF-1α was assayed by immunoblot at multiple time points after PDT. As shown in Figure 6A, HIF-1α expression was induced after 1 h post PDT. Then, CaCo2 cells were transiently transfected with shHIF-1α or control vector and LC3 conversion was evaluated by immunoblot following PDT. Interestingly, downregulation of HIF-1α decreases LC3-II conversion after PDT (Figure 6B). This suggests that PDT induces HIF-1α stabilization which, in turn, promotes autophagy. Then, we analyzed the role of VMP1 in PDT context. As shown in Figure 6C, VMP1 protein expression is induced after PDT. Also, we explored if VMP1 modulates PDT-induced autophagy. CaCo2 cells transiently co-transfected with RFP-LC3 and shVMP1-EGFP were treated with PDT and LC3 recruitment was analyzed by fluorescence microscope. As shown in Figure 6D, RFP-LC3 remains diffuse in cells expressing

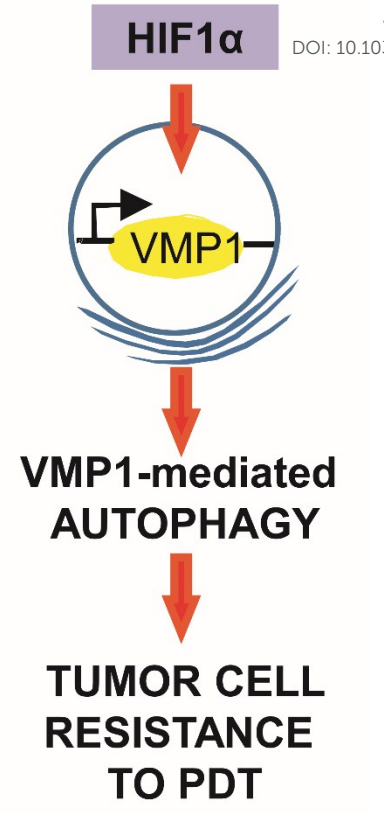

Figure 7. Schematic model. HIF-1α/VMP1-induced autophagy confers resistance to cell death under PDT.

shVMP1-EGFP compared to RFP-LC3 alone after PDT, indicating that VMP1-mediated autophagy is induced by PDT. Accordingly, as shown in Figure 6E, downregulation of VMP1 also decreased LC3 processing after PDT, which is similar to early stage inhibition of autophagy by 3-MA. These results indicate that PDT induces autophagy in a VMP1 dependent manner.

Finally, we evaluated the role of VMP1 in cell survival after PDT. Cells were transiently transfected with shVMP1-EGFP or shControl vector and cell viability was determined after PDT by MTT assay. As shown in Figure 6F, downregulation of VMP1 sensitizes cells to PDT. Together, these findings strongly suggest that HIF-1α/VMP1/autophagy pathway is induced by PDT and acts as a survival mechanism in colon cancer cells.

Discussion

Hypoxia is a widely studied factor promoting cancer cell chemo/radioresistance[40] and, in the last decade, it has been implicated in resistance to PDT protocols[41,42]. Autophagy has been also proposed as a common mechanism of resistance to chemotherapy and targeted therapies including PDT[43,21].
It was suggested that autophagy is a common response to PDT and that it is involved in either cell survival or cell death[21]. On the other hand, it was shown that PDT is able to induce stabilization and activation of HIF-1α[44]. Nevertheless, the implication of HIF-1 as modulator of autophagy in response to PDT has not been elucidated. Previously, we proposed possible

View Article Online
DOI: 10.1039/C7PP00161D

effects of PDT on tumor microenvironment, in which it is stated that HIF-1 might trigger autophagy as a survival mechanism[45]. Here, we show that colon cancer cells efficiently induce protein expression and transcriptional activity of HIF-1 under $CoCl_2$ treatment. Also, notable induction of autophagy is dependent of HIF-1α after $CoCl_2$ treatment suggesting that HIF-1 is an efficient player to modulate autophagy in colon cancer cells. Our results are consistent with reports suggesting that HIF-1 is able to induce autophagy[37,46] and other study suggesting that, in hypoxic-mimic conditions, cancer cells are more resistant to PDT in a HIF-1 dependent manner[42].

Our data reveal that HIF-1α is critical for $CoCl_2$-induced PDT resistance, since cancer cells incubated with $CoCl_2$ showed higher percentage of cell survival compared to control cells under PDT. Moreover, we demonstrated that $CoCl_2$ promotes resistance to PDT through autophagy induction, because the inhibition of autophagy under conditions where HIF-1α is stabilized, increases cell sensitization to PDT. We show that PDT induces a significant increase of autophagic flux in both CaCo2 and SW480 cells. Interestingly, when colon cancer cells were treated with autophagy inhibitors such as 3-MA, WM or CQ, the currently available autophagy pharmacological inhibitors[47], they become sensitive to PDT. The inhibitor 3-MA can affect cell survival in an autophagy independent manner through AKT and other kinases[48]. It has also been reported that CQ can inhibit cell growth and promotes cell death in cancer cells[49,50] . However, in our model conditions, we did not observe cytotoxic effects when colon cancer cells were treated with 3-MA, WM or CQ alone.

The autophagy-related protein VMP1 is required for autophagosome formation in mammalian cell in all conditions and its expression triggers autophagy even under nutrient-rich conditions[23,27]. VMP1 binds directly to BH3 domain of Beclin-1 promoting the dissociation of Bcl-2 from Beclin-1 and the activation of the Class III PI3K complex to initiate the autophagosome formation[25,26]. Previously, we demonstrated that VMP1 is induced by gemcitabine in pancreatic cancer cells[29] and that the AKT1-GLI3-VMP1 pathway mediates KRAS oncogene-induced autophagy in pancreatic cancer cells[28]. Other authors suggested that VMP1 expression can be also modulated by a HIF-1/miR-210 pathway in ovarian cancer cells[51]. Here we demonstrate that VMP1 is induced under HIF-1α stabilization. We found three HRE consensus sequences in position 59704668-59708628 on chromosome 17 of the human genome, which includes exon 1, intron 1 and 2800 bp 5´upstream sequence of exon 1, and ChIP assays show direct binding of HIF1α to VMP1 promoter. Our results indicate that VMP1 is a novel direct target of HIF-1α and its expression mediates HIF-1α-induced autophagy. Therefore, we propose a key role of HIF-1α in the initiation steps of VMP1-related autophagy in colon cancer cells.

It is possible that autophagy attempts to remove organelles damaged by oxidation or to degrade large aggregates of cross-linked proteins. Thus, ROS produced by the photodynamic treatment could be involved in autophagy induction[52]. PDT may result in a temporal photochemical consumption of molecular oxygen[53,54]. Moreover, PDT-induced ROS may evoke HIF-1α stabilization and activation[55,56,57]. In this sense, our results have demonstrated that PDT significantly increased the expression of HIF-1α in colon cancer cells. In addition, when HIF-1α is downregulated, cells become sensitive to PDT, indicating that PDT induces HIF-1α as a survival mechanism during treatment.

Together our results indicate that PDT, employing Me-ALA as photosensitizer, induces autophagy as a resistance mechanism. It has been showed that tumor resistance to PDT can be induced through upregulation of autophagy using other photosensitizers[58,59]. In this sense, while our results showed that HIF-1/autophagy can work together in our experimental conditions (CoCl2/PDT context), we cannot rule out the possibility that autophagy might be induced by HIF-1 independent mechanisms in response to PDT[60]. Further investigation on other mechanisms of resistance mediated by autophagy (e.g by rapamycin or cDNA-VMP1) in conditions where HIF-1 is downregulated would be of interest.

Finally, we demonstrated that HIF-1α and VMP1 are involved in PDT-induced autophagy. Our study showed that both HIF-1α and VMP1 are markedly increased following PDT. It is interesting to note that VMP1 kinetic-expression seems to be biphasic. This might be explained considering that VMP1 is a stress protein which is rapidly expressed by preformed RNA Moreover, downregulation of HIF-1α or VMP1 decreases LC3 processing and inhibit LC3 puncta formation after PDT, which confirm that HIF-1/VMP1 axis is required for PDT-induced autophagy. To our knowledge, this is the first report showing that PDT-induced autophagy is directly mediated by HIF-1α and linked to VMP1 as PDT-induced resistance mechanism.

Conclusions

The present study has demonstrated that PDT resistance in colon cancer cells under $CoCl_2$ treatment is mediated by the induction of a novel HIF-1α/VMP1/autophagy pathway, which could be exacerbated by PDT effects (Figure 7). Further studies focusing in the potential clinical application of this molecular mechanism of tumor cell resistance will provide novel strategies of PDT protocols for colon cancer.

Conflicts of interest

There are not conflicts of interest to declare.

Acknowledgements

Authors thank to Dr. Thomas Foster by provide the 5HRE-hCMV-d2EGFP plasmid, Dr. Eric Metzen by provide pLKO.1-shRNAHIF-1α-1 and PLKO.1-shScrambled plasmids and Dr. Edurne Berra by provide pcDNA3-HA-DN-HIF-1α plasmid.

1. Longo DL, Strum WB. Colorectal Adenomas. N Engl J Med. 2016;374(11):1065-1075.
2. De Greef K, Rolfo C, Russo A, et al. Multisciplinary management of patients with liver metastasis from colorectal cancer. World J Gastroenterol. 2016;22(32):7215-7225.
3. Heaney RM, Shields C, Mulsow J. Outcome following incomplete surgical cytoreduction combined with intraperitoneal chemotherapy for colorectal peritoneal metastases. World J Gastrointest Oncol. 2015;7(12):445-454.
4. Brown SB, Brown EA, Walker I. The present and future role of photodynamic therapy in cancer treatment. Lancet Oncol. 2004;5(8):497-508.
5. Oniszczuk A, Wojtunik-Kulesza KA, Oniszczuk T, Kasprzak K. The potential of photodynamic therapy (PDT)—Experimental investigations and clinical use. Biomed Pharmacother. 2016;83:912-929.
6. Castano AP, Demidova TN, Hamblin MR. Mechanisms in photodynamic therapy: part two—cellular signaling, cell metabolism and modes of cell death. Photodiag Photodyn Ther. 2005;2(1):1-23.
7. Yoo J-O, Ha K-S. New insights into the mechanisms for photodynamic therapy-induced cancer cell death. Int Rev Cell Mol Biol. 2012;295:139-174.
8. Shishkova N, Kuznetsova O, Berezov T. Photodynamic therapy in gastroenterology. J Gastrointest Cancer. 2013;44(3):251-259.
9. Barr H, MacRobert AJ, Tralau CJ, Boulos PB, Bown SG. The significance of the nature of the photosensitizer for photodynamic therapy: quantitative and biological studies in the colon. Br J Cancer. 1990;62(5):730-735.
10. Cosse J-P, Michiels C. Tumour hypoxia affects the responsiveness of cancer cells to chemotherapy and promotes cancer progression. Anticancer Agents Med Chem. 2008;8(7):790-797.
11. Balamurugan K. HIF-1 at the crossroads of hypoxia, inflammation, and cancer. Int J Cancer. 2016;138(5):1058-1066.
12. Michiels C, Tellier C, Feron O. Cycling hypoxia: A key feature of the tumor microenvironment. Biochim Biophys Acta - Rev Cancer. 2016;1866(1):76-86.
13. Amelio I, Melino G. The p53 family and the hypoxia-inducible factors (HIFs): determinants of cancer progression. Trends Biochem Sci. 2015;40(8):425-434.
14. Lin L, Baehrecke EH. Autophagy, cell death, and cancer. Mol Cell Oncol. 2015;2(3):e985913.
15. Harhaji-Trajkovic L, Vilimanovich U, Kravic-Stevovic T, Bumbasirevic V, Trajkovic V. AMPK-mediated autophagy inhibits apoptosis in cisplatin-treated tumour cells. J Cell Mol Med. 2009;13(9B):3644-3654.
16. Liu D, Yang Y, Liu Q, Wang J. Inhibition of autophagy by 3-MA potentiates cisplatin-induced apoptosis in esophageal squamous cell carcinoma cells. Med Oncol. 2011;28(1):105-111.
17. Del Bello B, Toscano M, Moretti D, Maellaro E. Cisplatin-induced apoptosis inhibits autophagy, which acts as a pro-survival mechanism in human melanoma cells. PLoS One. 2013;8(2):e57236.
18. Terman A, Brunk UT. Autophagy in cardiac myocyte homeostasis, aging, and pathology. Cardiovasc Res. 2005;68(3):355-365.
19. Yang X, Yu D-D, Yan F, et al. The role of autophagy induced by tumor microenvironment in different cells and stages of cancer. Cell Biosci. 2015;5(1):14.
20. François A, Marchal S, Guillemin F, Bezdetnaya L. mTHPC-based photodynamic therapy induction of autophagy and apoptosis in cultured cells in relation to mitochondria and endoplasmic reticulum stress. Int J Oncol. 2011;39(6):1537-1543.
21. O'Donovan TR, O'Sullivan GC, McKenna SL. Induction of autophagy by drug-resistant esophageal cancer cells promotes their survival and recovery following treatment with chemotherapeutics. Autophagy. 2011;7(5):509-524.
22. Wei M-F, Chen M-W, Chen K-C, et al. Autophagy promotes resistance to photodynamic therapy-induced apoptosis selectively in colorectal cancer stem-like cells. Autophagy. 2014;10(7):1179-1192.
23. Ropolo A, Grasso D, Pardo R, et al. The pancreatitis-induced vacuole membrane protein 1 triggers autophagy in mammalian cells. J Biol Chem. 2007;282(51):37124-37133.
24. Vaccaro MI, Ropolo A, Grasso D, Iovanna JL. A novel mammalian trans-membrane protein reveals an alternative initiation pathway for autophagy. Autophagy. 2008;4(3):388-390.
25. Molejon MI, Ropolo A, Vaccaro MI. VMP1 is a new player in the regulation of the autophagy-specific phosphatidylinositol 3-kinase complex activation. Autophagy. 2013;9(6):933-935.
26. Molejon MI, Ropolo A, Re A Lo, Boggio V, Vaccaro MI. The VMP1-Beclin 1 interaction regulates autophagy induction. Sci Rep. 2013;3:1055.
27. Grasso D, Ropolo A, Lo Ré A, et al. Zymophagy, a novel selective autophagy pathway mediated by VMP1-USP9x-p62, prevents pancreatic cell death. J Biol Chem. 2011;286(10):8308-8324.
28. Lo Ré AE, Fernández-Barrena MG, Almada LL, et al. Novel AKT1-GLI3-VMP1 pathway mediates KRAS oncogene-induced autophagy in cancer cells. J Biol Chem. 2012;287(30):25325-25334.
29. Pardo R, Lo Ré A, Archange C, et al. Gemcitabine induces the VMP1-mediated autophagy pathway to promote apoptotic death in human pancreatic cancer cells. Pancreatology. 2010;10(1):19-26.
30. Richard DE, Berra E, Pouyssegur J. Nonhypoxic pathway mediates the induction of hypoxia-inducible factor 1alpha in vascular smooth muscle cells. J Biol Chem. 2000;275(35):26765-26771.
31. Curtis MJ, Bond RA, Spina D, et al. Experimental design and analysis and their reporting: new guidance for publication in BJP. Br J Pharmacol. 2015;172(14):3461-3471.
32. Lopez-Sánchez LM, Jimenez C, Valverde A, et al. CoCl2, a Mimic of Hypoxia, Induces Formation of Polyploid Giant Cells with Stem Characteristics in Colon Cancer. Maki CG, ed. PLoS One. 2014;9(6):e99143.
33. LaGory EL, Giaccia AJ. The ever-expanding role of HIF in tumour and stromal biology. Nat Cell Biol. 2016;18(4):356-365.
34. Shibata T, Giaccia AJ, Brown JM. Development of a hypoxia-responsive vector for tumor-specific gene therapy. Gene Ther. 2000;7(6):493-498.
35. Kabeya Y, Mizushima N, Ueno T, et al. LC3, a mammalian homologue of yeast Apg8p, is localized in autophagosome membranes after processing. EMBO J. 2000;19(21):5720-5728.
36. Wilkinson S, O'Prey J, Fricker M, Ryan KM. Hypoxia-selective macroautophagy and cell survival signaled by autocrine PDGFR activity. Genes Dev. 2009;23(11):1283-1288.
37. Sun Y, Xing X, Liu Q, et al. Hypoxia-induced autophagy reduces radiosensitivity by the HIF-1α/miR-210/Bcl-2 pathway in colon cancer cells. Int J Oncol. 2015;46(2):750-756.
38. Gariboldi MB, Taiana E, Bonzi MC, et al. The BH3-mimetic obatoclax reduces HIF-1α levels and HIF-1 transcriptional activity and sensitizes hypoxic colon adenocarcinoma cells to 5-fluorouracil. Cancer Lett. 2015;364(2):156-164.
39. Klionsky DJ. The molecular machinery of autophagy: unanswered questions. J Cell Sci. 2005;118(Pt 1):7-18.
40. Brown JM, Wilson WR. Exploiting tumour hypoxia in cancer treatment. Nat Rev Cancer. 2004;4(6):437-447.
41. Ji Z, Yang G, Shahzidi S, et al. Induction of hypoxia-inducible factor-1alpha overexpression by cobalt chloride enhances cellular resistance to photodynamic therapy. Cancer Lett. 2006;244(2):182-189.

42. Casas A, Venosa G Di, Hasan T, Batlle A. Mechanisms of Resistance to Photodynamic Therapy. Current. 2011;(Ii):2486-2515.
43. Ma X-H, Piao S, Wang D, et al. Measurements of Tumor Cell Autophagy Predict Invasiveness, Resistance to Chemotherapy, and Survival in Melanoma. Clin Cancer Res. 2011;17(10):3478-3489.
44. Mitra S, Cassar SE, Niles DJ, Puskas JA, Frelinger JG, Foster TH. Photodynamic therapy mediates the oxygen-independent activation of hypoxia-inducible factor 1alpha. Mol Cancer Ther. 2006;5(12):3268-3274.
45. Milla Sanabria L, Rodríguez ME, Cogno IS, et al. Direct and indirect photodynamic therapy effects on the cellular and molecular components of the tumor microenvironment. Biochim Biophys Acta. 2013;1835(1):36-45.
46. Tittarelli A, Janji B, Van Moer K, Noman MZ, Chouaib S. The Selective Degradation of Synaptic Connexin 43 Protein by Hypoxia-induced Autophagy Impairs Natural Killer Cell-mediated Tumor Cell Killing. J Biol Chem. 2015;290(39):23670-23679.
47. Klionsky DJ, Abdelmohsen K, Abe A, et al. Guidelines for the use and interpretation of assays for monitoring autophagy (3rd edition). Autophagy. 2016;12(1):1-222.
48. Levine B, Yuan J. Autophagy in cell death: an innocent convict? J Clin Invest. 2005;115(10):2679-2688.
49. Maycotte P, Aryal S, Cummings CT, Thorburn J, Morgan MJ, Thorburn A. Chloroquine sensitizes breast cancer cells to chemotherapy independent of autophagy. Autophagy. 2012;8(2):200-212.
50. Fan C, Wang W, Zhao B, Zhang S, Miao J. Chloroquine inhibits cell growth and induces cell death in A549 lung cancer cells. Bioorg Med Chem. 2006;14(9):3218-3222.
51. Liu T, Zhao L, Chen W, et al. Inactivation of von Hippel-Lindau increases ovarian cancer cell aggressiveness through the HIF1α/miR-210/VMP1 signaling pathway. Int J Mol Med. 2014;33(5):1236-1242.
52. Scherz-Shouval R, Shvets E, Fass E, Shorer H, Gil L, Elazar Z. Reactive oxygen species are essential for autophagy and specifically regulate the activity of Atg4. EMBO J. 2007;26(7):1749-1760.
53. Foster TH, Murant RS, Bryant RG, Knox RS, Gibson SL, Hilf R. Oxygen consumption and diffusion effects in photodynamic therapy. Radiat Res. 1991;126(3):296-303.
54. Sitnik TM, Hampton JA, Henderson BW. Reduction of tumour oxygenation during and after photodynamic therapy in vivo: effects of fluence rate. Br J Cancer. 1998;77(9):1386-1394.
55. Jung S-N, Yang WK, Kim J, et al. Reactive oxygen species stabilize hypoxia-inducible factor-1 alpha protein and stimulate transcriptional activity via AMP-activated protein kinase in DU145 human prostate cancer cells. Carcinogenesis. 2008;29(4):713-721.
56. Lee JY, Hirota SA, Glover LE, Armstrong GD, Beck PL, MacDonald JA. Effects of Nitric Oxide and Reactive Oxygen Species on HIF-1a Stabilization Following Clostridium Difficile Toxin Exposure of the Caco-2 Epithelial Cell Line. Cell Physiol Biochem. 2013;32(2):417-430.
57. Li Y-N, Xi M-M, Guo Y, Hai C-X, Yang W-L, Qin X-J. NADPH oxidase-mitochondria axis-derived ROS mediate arsenite-induced HIF-1α stabilization by inhibiting prolyl hydroxylases activity. Toxicol Lett. 2014;224(2):165-174.
58. Dewaele M, Martinet W, Rubio N, et al. Autophagy pathways activated in response to PDT contribute to cell resistance against ROS damage. J Cell Mol Med. 2011;15(6):1402-1414.
59. Tu P, Huang Q, Ou Y, et al. Aloe-emodin-mediated photodynamic therapy induces autophagy and apoptosis in human osteosarcoma cell line MG-63 through the ROS/JNK signaling pathway. Oncol Rep. doi.org/10.3892/or.2016.4703
60. Choi H, Merceron C, Mangiavini L, et al. Hypoxia promotes noncanonical autophagy in nucleus pulposus cells independentof MTOR and HIF1A signaling. Autophagy. 2016;12(9):1631-46.

View Article Online
DOI: 10.1039/C7PP00161D

View Article Online
DOI: 10.1039/C7PP00161D

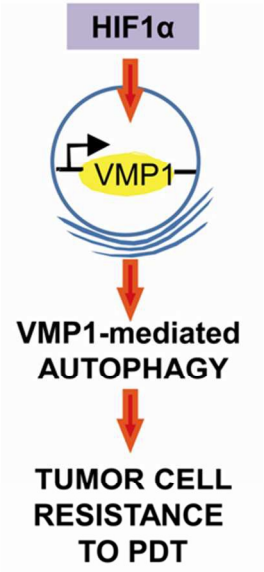

This is the first report showing that PDT-induced autophagy is directly mediated by HIF-1α and linked to VMP1 as PDT-induced resistance mechanism.

254x190mm (96 x 96 DPI)